

Changes in Holocene meridional circulation and poleward Atlantic flow: the Bay of Biscay as a nodal point

Mary, Yannick (1), Eynaud, Frédérique (1), Colin, Christophe (2), Rossignol, Linda (1), Brocheray, Sandra (1, 3), Mojtahid, Meryem (4), Garcia, Jennifer (4), Peral, Marion, (1, 5), Howa, Hélène (4), Zaragosi, Sébastien (1), Cremer, Michel (1)

(1) *Laboratoire Environnements et Paléoenvironnements Océaniques et Continentaux (EPOC) -UMR 5805, Université de Bordeaux, 33615 Pessac, France*

(2) *Laboratoire Géosciences - Université de Paris-Sud, 91405 Orsay Cedex, France*

(3) *now at: Institut Polytechnique LaSalle-Beauvais – Dpt Géosciences, 19 rue Pierre Waguët – BP 30313 – 60026 Beauvais, France*

(4) *UMR CNRS6112 LPG-BIAF, Recent and Fossil Bio-Indicators, Angers University, 2 Bd Lavoisier, 49045 Angers CEDEX 01, France*

(5) *now at Laboratoire des Sciences du Climat et de l'Environnement (LSCE-IPSL), Domaine du CNRS, bât.12 - 91198 Gif-sur-Yvette, France*

Keywords

Meridional circulation, Bay of Biscay, Holocene, Sea surface temperature, North Atlantic, Subpolar and Subtropical Gyres

Abstract

This paper documents the last 10 ka evolution of one of the key parameters of climate: sea-surface temperatures (SST) in the North Atlantic. We focus on the southern Bay of Biscay, a highly sensitive oceanographic area regarding the dynamics of the North Atlantic subpolar and subtropical gyres (SPG and STG respectively). This site furthermore offers unique sedimentary environments characterized by exceptional accumulation rates, enabling the study of Holocene archives at (infra)centennial scales. Our results mainly derive from planktonic foraminiferal association analysis on two cores from the southern Landes plateau. These associations are used as the basis of Modern Analogue Technique transfer functions to track past hydrographical changes. SST reconstructions were thus obtained at an exceptional resolution and compared to a compilation of Holocene records from the north-eastern North Atlantic. From this regional perspective are shown fundamental timing differences between the gyre dynamics, nuancing classical views of a simple meridional overturning cell. Our study highlights that western Europe underwent significant oscillations of (annual) SST during the last 10 ka. During well known intervals of mild boreal climate, warm shifts of more than 3°C per centuries are accurately concomitant

35 with positive sea-surface temperature anomalies and rise of micropaleontological indicators of gyre
36 dynamics in the northern North Atlantic, pointing to periods of greater intensity of the North Atlantic
37 Current (SPG cell especially) . Conversely, SST signal records short-term cold anomalies which could be
38 related to weaker SPG dynamics.

1. Introduction

The Atlantic Meridional Overturning Circulation (AMOC) and its dynamics are critical regarding the modulations of climate (amplitude and frequency) over Europe (westerlies, droughts and/or stormy periods, e.g. Clark et al., 2002; Bryden et al., 2005; Dawson et al., 2004; Magny et al., 2003; Sorrel et al., 2009; Trouet et al., 2012, Van Vliet-Lanoe et al., 2014a and b, Jackson et al., 2015). The two connected North Atlantic gyres, the subpolar gyre (SPG) and the subtropical gyre (STG) are fundamental for these processes as they transfer heat and salt toward the Nordic seas (e.g., McCartney and Mauritzen, 2001; Perez-Brunius et al., 2004; Hatun et al., 2005; Morley et al., 2014) where convection occurs (e.g. Lozier and Stewart, 2008). Their expansions and contractions notably control the inflow from the North Atlantic Current (NAC) to higher latitudes, thus also affecting the heat budget of the Greenland-Iceland-Norwegian seas, which is critical in the meridional climatic balance (i.e., Hatun et al., 2005). During the late Holocene, changes in the STG and SPG dynamics contributed to well-known climatic anomalies in Western Europe, such as the Little Ice Age or the Medieval Warm Period/Anomaly, and probably played a major role at longer time scales (Thornalley et al., 2009; Colin et al., 2010; Copard et al., 2012; Sorrel et al., 2012; Staines-Urias et al., 2013; Morley et al., 2014;).

By providing the first Holocene inventory of (infra)centennial hydrographic changes in the inner Bay of Biscay, this paper aims at testing European temperate oceanic signals vs. those from a broader North Atlantic view with a focus on the SPG dynamics. Our study site (Figure 1) is ideally located under the temperate eastern limb of the NAC, in the southern Bay of Biscay and not far from the STG/SPG divergence zone (e.g. Planque et al., 2003). This geographic configuration provides to this marine environment a high sensitivity regarding Northern hemisphere climatic signals at present (e.g. Le Cann and Serpette, 2009; Esnaola et al., 2012; Garcia-Soto and Pingree, 2012), echoing pan-Atlantic hydrographical changes, somewhat with amplified responses. Actually, the southern Bay of Biscay records at present the warmest SST (especially in summer) of the mid-latitude temperate band of the North Atlantic with a significant warming trend over the last decades (e.g. Koutsikopoulos et al., 1998; Valencia et al., 2003; deCastro et al., 2009, see also maps at <http://www.nodc.noaa.gov/cgi-bin/OC5/woa13fv2/woa13fv2.pl?parameter=t>). Previous works done on sedimentary archives in the same

66 area have furthermore evidenced a strong potential to track down the Holocene variability (Mojtahid et
67 al., 2013; Garcia et al., 2013; Brocheray et al., 2014; Mary et al., 2015).

68 Today, the Bay of Biscay is characterized by a complex, variable sea-surface circulation with
69 strong seasonal changes, marked by a September-October versus March-April - *SOMA* pattern (e.g.,
70 Pingree and Lecann, 1990; Pingree and Garcia-Soto, 2014). The main surface current in the Bay of
71 Biscay is the European Slope Current (ESC), flowing northward along the Armorican Shelf ([Figure 1](#)),
72 with important spatial and seasonal variations (Garcia-Soto and Pingree, 2012; Charria et al., 2013).
73 Circulation can reverse during summer along the shelf break, flowing weakly southwestward (Charria et
74 al., 2013). In autumn-winter, the northward flow reaches a maximum, especially when combining with
75 southern intrusions from the Iberian Poleward Current (IPC) which flows along the western Iberian
76 margin (e.g. Peliz et al., 2005) before turning eastward at the Cape Finisterre (NW Spain). The IPC
77 northward extension into the Bay of Biscay is known as the Navidad Current (e.g. Garcia-Soto et al.,
78 2002; Le Cann and Serpette, 2009). The winter mixing of the IPC and ESC is designated as the European
79 Poleward Current (EPC, Garcia-Soto and Pingree, 2012), and drives relatively warm and saline water to
80 the Nordic seas, contributing to their heat and salt budget. The Bay of Biscay is additionally strongly
81 marked by surface water inflow coming from the North Atlantic Current ([Figure 1](#)), which enters the Bay
82 from its northwestern boundary (Pingree, 2005; Pingree and Garcia-Soto, 2014; Ollitrault and Colin de
83 Verdier, 2014). In contrast with surface circulation of the inner Bay of Biscay, the NAC water inflow
84 shows only limited seasonal variability. At inter-annual time scales however, NAC oscillations are mainly
85 driven by westerly wind regime (Pingree, 2005), and consequently by the North Atlantic Oscillation
86 (NAO), one of the key modes of climatic variability in the North Atlantic. So far, little is known about
87 long term oscillations of the NAC inflow into the Bay. Modern surveys of SST variability over the last
88 150 years in the Bay of Biscay report that temperature oscillations are mainly controlled by the Atlantic
89 Multi-decadal Oscillation (AMO, Garcia-Soto and Pingree, 2012). The influence of the NAO on SST in
90 the Bay of Biscay is more complex and contributes only little to the observed long term trend, although
91 sharp, inter-annual changes of the NAO index impact annual SST variability (Garcia-Soto and Pingree,
92 2012, [Figure 1C](#)). Moreover, NAO conditions influence large-scale oceanic circulation patterns indirectly

93 responsible for surface temperature anomalies over the Bay (Pingree, 2005; Garcia-Soto and Pingree,
94 2012, see also the synthesis within Mary et al., 2015).

95 The present paper is based on analyses conducted on two high-resolution well dated cores from
96 the southern part of the inner Bay of Biscay (Figure 1, Table 1): core KS10b (e.g. Mojtahid et al., 2013)
97 and core PP10-07 (e.g. Brocheray et al., 2014). These cores show exceptionally high sedimentation rates
98 for the Holocene, up to 200 cm.ka⁻¹ for core PP10-07, and 86 cm ka⁻¹ for core KS10b (see detailed
99 description of these archives and of their sedimentological context in the respective references). Here we
100 present past Holocene SST data reconstructed after an ecological transfer function based on the Modern
101 Analogue Technique (see Methods) applied to planktonic foraminiferal assemblages. These Bay of
102 Biscay sea-surface reconstructions are compared to selected North Atlantic Holocene records using a data
103 mining exercise (referencing sea-surface reconstructions of high time-resolution) done in the frame of the
104 French ANR HAMOC (Holocene North Atlantic Gyres and Mediterranean Overturning dynamic through
105 Climate Changes) project database (see <http://hamoc-interne.epoc.u-bordeaux1.fr/doku.php?id=start>) .
106

107 2. Methods

108 2.1. Age models

109 Updated age models have been built for the Bay of Biscay cores. All raw ¹⁴C ages were calibrated
110 and converted to calendar ages using the Marine13 calibration curve and the recommended age reservoir
111 of 405 years (Reimer et al., 2013), as no adequate and robust local age reservoir values exist in the area
112 (see Mary et al., 2015 for a discussion). Smooth-spline regression based on the published ¹⁴C dates (n =12
113 for core Ks10b, Mojtahid et al., 2013) were applied (Figure 2). For core PP10-07, two supplementary ¹⁴C
114 dates were obtained at the top of the sequence (Table 2) and the age model was built using a 5 degree
115 polynomial regression (Figure 2). Core MD03-2693 age model (also exploited in this paper) was built
116 using linear interpolation based on published ¹⁴C and ²¹⁰Pb (n=3 and n=8, respectively, Mary et al., 2015).
117 Age-depth modeling and calibration were performed using the dedicated software Clam (Blaauw, 2010),
118 written in the open-source statistical environment R (<http://www.r-project.org/>).

2.2.Past hydrographical parameter quantification

Planktonic foraminifera (PF) assemblages were used to quantify sea-surface parameters: species abundances were determined (counts of 300 specimens at least) on the $> 150 \mu\text{m}$ fraction from sedimentary aliquots retrieved at maximum 10 centimeter-intervals along the studied cores, thus giving a mean time resolution of 50 and 150 years for core PP10-07 and KS10b respectively (see Supplementary material for detailed data). SST reconstructions were calculated using the Modern analogue technique (MAT) a method successfully developed on PF (e.g., Pflaumann et al., 1996; Kucera et al., 2005; Telford and Birks, 2011; Guiot and de Vernal, 2007; 2011). The calculations derive from modern spectra previously compiled and tested separately in the frame of the MARGO exercise for the North Atlantic Ocean and the Mediterranean Sea respectively (Kucera et al., 2005; Hayes et al., 2005). They are based on sediment surface samples analyzed for their contents in PF (specific relative abundances) and thus offer the advantage of already having integrated regional taphonomic processes. At EPOC (Environnements et Paléoenvironnements Océaniques et Continentaux) laboratory, these two MARGO databases were summed to provide larger analogue choices and ambiguous data points were excluded (i.e. non-stratigraphically constrained points showing anomalies in the biogeographical distribution), resulting in a final training set of $n=1007$ modern analogues. Modern sea-surface parameters were extracted from the WOA ATLAS with the sample tool developed by Schäfer-Neth and Manschke (2002). The latter was developed for the MARGO program and interpolates the 10 m World Ocean Atlas WOA -1998 mean seasonal and mean annual temperatures over the four existing data points surrounding the sample location (see <http://www.geo.uni-bremen.de/geomod/staff/csn/woasample.html>) thus providing spatio-temporal averaged values of SST (see Kucera et al., 2005 for MARGO analytical developments and Telford et al., 2013 for further considerations).

Calculations were run under the R software with the BIOINDIC package (ReconstMAT script) developed by J. Guiot (<https://www.eccorev.fr/spip.php?article389>) using relative abundances of PF with no

144 mathematical transformation (no logarithmic or square root transformations which are frequently used to
145 increase the equitability within assemblages for instance, see Guiot and de Vernal, 2007 for a review).
146 Past hydrological parameter values are derived from a weighted average of the SST values of the five best
147 analogues. The maximum weight is given for the closest analogue in terms of statistical distance (i.e.
148 dissimilarity minimum). The ReconstMAT script furthermore includes the calculation of a threshold
149 regarding this statistical distance which prevents calculation in the case of poor- or non- analogous
150 situations. The degree of confidence of this method allows reconstruction of seasonal and annual SST
151 with a maximum root mean square error of prediction (RMSEP) of 1.3°C (see Supplementary material).
152 This method (named MATR_1007PF for Modern Analogue Technique derived from 1007 modern
153 spectra of PF assemblages) was extensively tested at EPOC including comparisons with similar MAT
154 developed regionally on PF (e.g. Salgueiro et al., 2008; 2010) providing very coherent reconstructions
155 along the western European margin (see Eynaud et al., 2013 for further details) and producing pertinent
156 paleoceanographical series (see Penaud et al., 2011; Sánchez Goñi et al., 2012; Sánchez Goñi et al., 2013
157 for records also produced with MATR_1007PF). Additionally, our work benefited from modern
158 calibrations conducted on PF from the same area of the Bay of Biscay (i.e. Retailleau et al., 2009; 2012).

160 **3. Holocene SST oscillations in the Bay of Biscay**

161 Despite the different bathymetric and physiographic positions of the studied cores (Figure 1, Table
162 1), reconstructed annual SST in the Bay of Biscay show coherent oscillations of remarkably similar
163 timing (Figure 3a). Small amplitude differences are observed between the two studied records, but
164 synchronous warm periods are clearly identified between 8.2-7.4 ka BP and 6.6-5.6 ka BP, these intervals
165 roughly corresponding to the upper and lower limits of the mid-Holocene hypsithermal in the North
166 Atlantic region (e.g. Eynaud et al., 2004; Walker et al., 2012; Tanner et al., 2015).

167 On historical time-scales, warm intervals are detected in both cores between 2.6-1.8 ka BP
168 (Roman Warm Period, RWP) and 1.2-0.5 ka BP (Medieval Warm Period, MWP), although less obvious
169 in core KS10b because of the lower time resolution. An offset of up to 4°C above mean annual modern
170 values is observed during a large temperature excursion around ca 2 Ka BP in core PP10-07 only. The

171 amplitude of the warmings detected between 8.2-7.4 ka BP and 6.6-5.6 ka BP reaches 2 to 3°C in both
172 records. Such amplitudes in the detected SST warm pulses are especially high in comparison to modern
173 annual values. However, considering the strong modern seasonal SST variations in the Bay of Biscay (as
174 shown on [Figure 3a](#)), a 4°C shift of mean annual SST is coherent with a deviation of annual mean
175 temperature toward mean summer values.

176 Comparison of the southern Bay of Biscay SST reconstructions with other records from the
177 Western European margin ([Figure 3, 4 and 5](#)) suggests that the observed millennial-scaled warm episodes
178 are coherent features which reflect characteristic climatic patterns, at least expressed regionally, but also
179 probably more broadly. Indeed, further along the Bay of Biscay margin, other high resolution Holocene
180 archives reveal similar and synchronous episodes ([Figure 3C](#)). Concomitantly to the observed warm SST
181 pulses also seen within the seasonal means (see Supplementary material), Holocene pollen assemblages
182 from core VK03-58 bis (pollen data not shown, Naughton et al., 2007a) indicate a decrease in mean
183 annual precipitations; this drought being related, according to the authors, to a change in the seasonality
184 with warmer summers especially. In the same way, the evolution of coccolithophorid concentrations in
185 the subpolar North-Atlantic along the Irminger Current pathway, interpreted as indicating stronger
186 contribution of NAC water toward the Nordic seas (Andrews and Giraudeau, 2003; Giraudeau et al.,
187 2004, Moros et al., 2012), showed strong similarities with the Bay of Biscay SST signals. Peaks in
188 coccolithophorid abundances in cores B997-330 and MD99-2269 ([Figure 4e and f](#)) (see location on
189 [Figure 1](#)) were recorded synchronously to the warm pulses in the Bay of Biscay, with especially
190 positively marked anomalies detected around 2 ka BP and 8 ka BP. The Bay of Biscay SST oscillations
191 further correspond with those reconstructed from marine records from the Barents Shelf (see location on
192 [Figure 1](#)) from core MSM5/5-712-2 (Werner et al., 2013, [Figure 3c](#)) and core M23258 (Sarnthein et al.,
193 2003; [Figure 3d](#)). This coherency suggests teleconnections between the southern Bay of Biscay and the
194 Nordic seas, probably due to a common driving mechanism linked to the NAC inflow vigor and its split
195 between the SPG and the STG.

196 In between the observed warm intervals, SST reconstructions of core PP10-07 and KS10b reveal
197 several low values slightly colder than today ([Figure 3a](#)). The time interval between 5.6 and 2.6 ka BP is

198 characterized by temperatures around -1°C cooler compared to the modern ones. This period roughly
199 corresponds to the late Holocene Neoglacial Cooling (e.g. Eynaud et al., 2004; Wanner et al., 2008;
200 Walker et al., 2012). In the same way, short-lived events of 2°C cooling are visible around ca 8.2, 7, 5.5,
201 4, 2.9 and 1.7 ka BP (Figure 3 and 4). The three older anomalies are synchronous and well-marked in
202 both KS10b and PP10-07 cores.

203 The comparison of the timing of these cold spells to other existing Holocene reconstructions from
204 the North Atlantic Ocean reveals that they represent coherent and reproducible features (Figure 4).
205 Interestingly, density anomalies thought to reflect millennial-scale variability in the SPG dynamics
206 (Thornalley et al., 2009; Farmer et al., 2011) were recorded nearly synchronously (within the age model
207 uncertainties) in the southern Iceland basin (it is especially obvious before 4ka). These anomalies were
208 interpreted (i.e. Thornalley et al., 2009) as reflecting a strong */weak*, longitudinally extended/*contracted*
209 SPG thus driving more/*less* vigorous but fresher/*saltier* Atlantic inflow throughout the Faroe current
210 branch and thus modulating the AMOC strength. The good temporal correspondence between the cold
211 spells detected in core PP10-07 (even if shorter) and the density anomalies (core RAPiD-12-1K, Figure
212 4h) registered in the subpolar North-Atlantic support, as seen for warm events, a direct teleconnection
213 with the inner Bay of Biscay, probably throughout a STG/SPG seesaw which would influence
214 tracks/intensities of the temperate westerlies. The short lived cold anomalies of PP10-07 are furthermore
215 concomitant with periods of increased storminess identified in various coastal sediments from the NW
216 European margin (Holocene Storm Periods after Sorrel et al., 2012, Figure 3g). These periods have been
217 related to a weakened, westward contracted SPG, involving a rapid feedback in the atmospheric dynamics
218 (e. g. westerlies intensity and/or latitudinal migrations).

219 In the subtropical North Atlantic, study of benthic foraminiferal stable isotopes in core EUGC-3B
220 (located in the Galician Shelf, Pena et al., 2010; see Figure 1) also showed similar cold anomalies which
221 were interpreted by the authors as suggesting enhanced contribution of colder, NE Atlantic ENACW
222 waters reaching the Iberian margin during these events.

4. The European poleward current and the influence of subtropical sourced waters in the Bay of Biscay

Modern surveys (e.g. Garcia-Soto et al., 2002; Lozier and Stewart, 2008; Garcia-Soto and Pingree, 2012) and paleoceanographic time-series (e.g., Mojtahid et al., 2013) recently evidenced the influence of the IPC, and its extension in the Bay of Biscay (i.e. Navidad Current, Garcia-Soto et al., 2002), on surface circulation and hydrological conditions along the European Margin. At present, these incursions of warm waters in the bay occur during winter under specific seasonal wind regimes (of southerly wind off Portugal and westerly wind off Northern Spain, Charria et al., 2013) and negative anomalies of sea level pressure over the North Atlantic (Pingree and Garcia-Soto, 2014). While these conditions were previously related to a negative mode of the NAO (Garcia-Soto et al., 2002), recent analysis of instrumental time-series showed that weather conditions responsible for Navidad current may not always correspond to a fixed value of the NAO index (Pingree and Garcia-Soto, 2014). The Navidad Current occasionally creates warm SST anomalies, enhanced transport of warm water through the pole and could thus be the vector of planktonic exotic (from subtropical origin) faunal invasions in the inner Bay of Biscay (see Mojtahid et al., 2013 and Garcia et al., 2013 for example in the fossil record; see Garcia-Soto and Pingree, 2012 and Pingree and Garcia-Soto, 2014 for example in instrumental time-series) which could bias our SST reconstructions. In the following, we thus examine the hypothesis of a persistent poleward surface current during the Holocene that would have triggered the observed SST warm anomalies in the PP10-07 and KS10b records.

In order to test the coherency of surface hydrographic features along the temperate and subtropical adjacent portions of the European margin, we compared Bay of Biscay SST reconstructions with existing SST (annual) records produced along the Iberian Margin (Figure 3b and c). We first test this link over historical times, compiling SST high resolution data obtained on the proximal core MD03-2693 (after Mary et al., 2015), which accurately complete those from core PP10-07 (see Figure 3a between 0.5 and 1.5 ka and Figure 5a', even if the cores are not tuned on each other's, i.e. keeping their independent age models; see also - AC2: 'Author Comment to Ref#2', Frederique Eynaud, 08 Dec 2016 and its cp-2016-32-supplement), with additional high resolution records (Figure 3b). The combination of these records reveals a slight warming associated to the Medieval Warm Period and coherent low-amplitude multi-decadal SST

251 oscillations which echoes those of AMO anomalies as reconstructed by Mann et al (2009). Especially
252 striking is the high degree of synchronicity detected between the Iberian margin (core PO287-06 , Abrantes
253 et al., 2011) and the Bay of Biscay at the scale of the last 1.5 ka, despite differences in the proxies used to
254 generate paleo-SST (Alkenones vs MAT on PF respectively) and age-model uncertainties (which probably
255 explain offsets of a few hundred years around 1200 A.D.). The good coherency with AMO reconstructions
256 further supports modern oceanographic assumptions of AMO driving multi-decadal change of SST in the
257 area (Garcia-Soto and Pingree, 2012) and shows that this modulation is at least valid for the late Holocene.
258 Interestingly, modern winter incursions of Iberian water through the Bay of Biscay take place during periods
259 of increasing AMO (Garcia-Soto and Pingree, 2012). During these episodes, warm winter anomalies of up to
260 1.1°C are observed in the Bay of Biscay, which are consistent with the amplitude of the warmings detected
261 in both MD03-2693 and PP10-07 past reconstructions.

262 However, over the longer Holocene perspective, existing SST records from the Iberian margin do
263 not reveal any coherent patterns with those from the Bay of Biscay over the last 10 ka (Figure 3c).
264 Regardless of the proxies involved in SST reconstructions (Alkenones and MAT), there is no evidence of
265 any earlier distinct SST excursions in the high time resolution data of the Iberian cores MD99-2331,
266 D13882, MD95-2042 and MD01-2444 (Figure 3c, see also Figure E4 in the Supplementary material) or
267 elsewhere in other lower resolution Holocene records from the same area (Naughton et al., 2007b; Martrat
268 et al., 2007; Rodrigues et al., 2009; Voelker and de Abreu, 2011; Chabaud et al., 2014). The early
269 Holocene SST reconstructions in this area show a monotonous long term decrease of SST correlated with
270 the Holocene decline of summer insolation (e.g. Marchal et al., 2002, see also Figure E4) which contrasts
271 strongly with the warm episodes observed in core PP10-07 and KS10b at that time (see Figure E4 in the
272 Supplementary material). Taking into account the similarities between late Holocene records in the
273 Iberian margin and in the Bay of Biscay, our data thus suggests a disconnection between these two
274 regions during the first part of the Holocene, up to 1.5 ka BP. We interpret this divergence as a distinct
275 response of the Bay of Biscay to North Atlantic millennial changes in the NAC/SPF system dynamics
276 (e.g. Perez-Brunius et al., 2004) whereas southwestern Europe has probably undergone a mixed influence
277 of diverse subtropical climatic trends. Sea-surface environments from the Bay of Biscay, located at the

278 interface between the SPG and STG influences may have, as currently observed in frontal regions,
279 recorded an amplified signature of NAC shifts, themselves driven by contraction/extension phases of the
280 whole North-Atlantic gyre system (STP, SPG, and Polar Gyre also). To decipher the role of each of these
281 gyres is at present not possible on the basis of our records only, and requires additional high-resolution
282 comparable marine archives along a latitudinal gradient at least between 30° and 60°N. The analyses of
283 the influence of Mediterranean hydrographic changes (via the Mediterranean outflow export especially)
284 together with those linked to the Eastern North Atlantic Upwelling Region would also be very important
285 to tackle in such a context.

287 **5. Implication for Holocene climate dynamics**

288 In agreement with modern climate observations (e.g. Ba et al., 2014), North Atlantic paleoceanographic
289 studies describe a strong impact of the Subpolar gyre (SPG) dynamics on the NAC inflow toward high-
290 latitudes and global circulation during the Holocene (Bianchi and Mc Cave, 1999; Oppo et al., 2003;
291 Perez-Brunius et al., 2004; Thornalley et al., 2009; Giraudeau et al., 2010; Moros et al., 2012; Staines-
292 Urías, 2013; Morley et al., 2014). Freshwater fluxes in the Labrador Sea and wind stress over the North
293 Atlantic are key drivers of eastern expansions/contractions of the SPG (Hatun et al., 2005), thus also
294 controlling the salinity balance over the North Atlantic, boreal deep-water convection and North
295 hemisphere climate patterns. The compilation of proxy-records from further south in the Bay of Biscay
296 indicates that the Holocene relatively long-term periods of warming are interbedded/superposed to rapid,
297 millennial cold anomalies of SPG origin (Figure 4). In agreement with other North Atlantic records,
298 strong NAC occurs preferentially during the Holocene optimum (Berner et al., 2007; Solignac et al.,
299 2008), and during the Roman Warm Period (Werner et al., 2012). In contrast, the occurrences of cold
300 anomalies in the North Atlantic follow a 1500 years periodicity during the Holocene (e.g., Thornalley et
301 al., 2009; Debret et al., 2007; Sorrel et al., 2012), and are accurately reflected by the SST PP10-07 record
302 (Figure 4f).

303 As also suggested by recent studies of modern time-series (Lozier et al., 2010; Lozier, 2012), Holocene
304 SST records from the Bay of Biscay evidence a decoupling of gyre dynamics, and a potential gyre-
305 specific expression of the AMOC. Model studies similarly question the meridional coherence of the
306 AMOC, revealing an inherent character of its mid-latitude variability at decadal time-scales (Bingham et
307 al., 2007), mainly driven by wind forcing and eddy variability. While our findings support coherent sea-
308 surface hydrographical patterns between subtropical and temperate environments along the western
309 European margin, suggesting a coupled SPG/STG gyre dynamics over the last 1.5 to 2 ka, earlier
310 Holocene contexts seem to have been rather favorable to a gyre-specific expression, i.e. each gyre being
311 related to intrinsic forcing mainly due to their latitudinal position and to proximal saline/fresh water
312 intrusions.

313 To tentatively go further in the interpretations, we have compiled bibliographic sources dealing with the
314 Holocene climatic variability. Many of the relevant records are considered on [Figures 4 and 5](#), with a
315 zoomed representation over the last 4 ka in [Figure 5\(5a' to 5e'\)](#) which gathers proximal European records.
316 Related interpretations and elements regarding the SPG/STG (and other ocean and climate features when
317 existing) were also compiled as a Table (see [Table E2](#) in Supplementary material) to provide a
318 comprehensive summary which is conceptualized on [Figure 6](#). With this exercise, is confirmed that no
319 definitive trend could be assessed over the whole Holocene. It seems rather that the delimitation of the
320 mid-Holocene is of high relevance regarding the latitudinal coherence of climatic events. Probably in
321 relation with the influence of relict ice-sheet melting (and thus fresh-water injection in the SPG) and the
322 related sea-level rise stop, key connections and feedbacks may have took place after 6/5 ka only, thus
323 triggering modern oceanographic and climatic modes. Actually, when focusing on the early Holocene,
324 warm anomalies in the Bay of Biscay coincide with signals of significant NAC inflow in the GIN seas
325 ([Figures 4 and 6a](#)), but are not clearly seen on records close from European ice-sheets ([Figure 5e](#)). At a
326 millennial scale, these events seem to be in phase with evidences of solar activity changes ([Figure 5f](#) –
327 reverted scale) and important pulses of ice-drifting in the North Atlantic (after Bond et al., 2001, [Figure](#)
328 [5g](#)). The centennial evolution within each event is however more complex. Over the last 5 ka, trends seem
329 to be more clearly expressed with, especially during the last millennia, good coherency at the local and

330 regional scales (Figure 5a' to 5e'). Warm/cold shifts occur in a well-defined temporal frame, relevant at
331 least over Europe, but hardly attributable on the basis of our work to a preferential radiative forcing
332 (internal as external).

333 To understand climatic processes behind these observations and test their coherency region per region, a
334 pan-(North)-Atlantic view is however required, emphasizing the need for comprehensive data
335 compilation efforts as those undertaken for instance in the work conducted for the Ocean2k SST synthesis
336 (e.g. McGregor et al., 2015) or the PAGES 2K Network consortium
337 (<http://pastglobalchanges.org/ini/wg/2k-network/intro>). SST records should however be supplemented by
338 complementary parameters when possible, especially to document hydrographic processes at various
339 depths, in order to better understand the 3D articulation of the oceanic thermal and dynamic responses to
340 various Holocene forcing (e.g. changes in insolation, sea-level - gateway connection, volcanism, or even
341 anthropogenic related, which could have been cumulative or not).

343 6. Conclusion

344 Our study, which documents Holocene surface hydrographical changes at unprecedented time-
345 scales in the Bay of Biscay, reveals contrasted patterns (warm vs cool SST) which correlate with other
346 North Atlantic proxy records interpreted to be responding to North Atlantic gyre dynamics. Coherently
347 with stronger NAC inflow in the Nordics seas as detected in other archives from the northern North
348 Atlantic, our high-resolution sedimentary records identify specific warm periods during the early
349 Holocene and at ca. 2 ka BP and reveal that northward advection of subtropical waters may have
350 influenced SST oscillations in the Bay of Biscay during the last 1.5 ka BP. In addition, SST signals from
351 the Bay of Biscay show the occurrences of short-term cold anomalies, interpreted here as the signature of
352 changes in SPG dynamics. The influence of the two main North Atlantic gyres, i.e STP vs SPG, observed
353 asynchronously over most of the Holocene in the Bay of Biscay, indicate fundamental differences in the
354 temporal variability of their dynamics, contrasting with the idea of a coherent, basin-wide-driven,
355 overturning cell in the North-Atlantic. Our results suggest a gyre-specific expression of the AMOC where
356 intrinsic salinity valves, linked to the latitudinal and geographical contexts, are of major importance. That

357 may contribute to strong regionalisms in the response of the North Atlantic hydrography to Holocene
358 climatic changes and imply to be as precise as possible when modeling this key component in the Earth
359 climate system. This urges also for a densification (and maybe diversification) in the coverage of past
360 Holocene archives.

362 7. Acknowledgments

363 Analyses documented in this study have been supported by the French ANR HAMOC. We are
364 grateful to the captain and crew of the RV *Pourquoi Pas?* and to the scientific team of the 2010-
365 SARGASS cruise. This work benefited from ^{14}C AMS measurement facilities thanks to the ARTEMIS
366 French project. We thank Giovanni Sgubin, Didier Swingedouw and Eleanor Georgiadis for useful
367 discussions and comments on the manuscript. This is an UMR EPOC contribution. Data will be set on
368 <http://www.pangaea.de/>.

369
370 M.Y. and E.F. designed the study and wrote the paper in the frame of the ANR HAMOC project
371 coordinated by C.C..

372 E.F., R.L., M.M., G.J., P.M., H.H. performed and/ or supervised planktonic foraminifera assemblage
373 analyses and picking for the datings. E.F. ran the transfer function. M.Y. performed age modelling with
374 the help of E.F. and M.M.. B.S, S.Z. and C.M. investigated the sedimentology of core PP10-07. All
375 authors contributed to discussions and interpretation of the results. The authors declare no competing
376 financial interests.

8. References

- Abrantes, F., Rodrigues, T., Montanari, B., Santos, C., Witt, L., Lopes, C., Voelker, A.H.L., 2011. Climate of the last millennium at the southern pole of the North Atlantic Oscillation: An inner-shelf sediment record of flooding and upwelling. *Climate Research* 48, 261–280.
- Andrews, J.T. and Giraudeau, J.: Multi-proxy records showing significant Holocene environmental variability: the inner N. Iceland shelf (Hunafloi), *Quaternary Science Reviews* 22, 175–193, 2003.
- Ba, J., Keenlyside, N. S., Latif, M., Park, W., Ding, H., Lohmann, K., Mignot, J., Menary, M., Otterå, O. H., Wouters, B., Salas y Melia, D., Oka, A., Bellucci, A., and Volodin, E.: A multi-model comparison of Atlantic multidecadal variability, *Climate Dynamics* 43, 2333–2348, 2014.
- Berner, K.S., Koç, N., Godtlielsen F., and Divine, D.: Holocene climate variability of the Norwegian Atlantic Current during high and low solar insolation forcing, *Paleoceanography* 26, n/a–n/a., 2011.
- Bianchi, G.G. and Mc Cave, I.N.: Holocene periodicity in North Atlantic climate and deep-ocean flow south of Iceland, *Nature* 397, 515–517, 1999.
- Bingham, R.J., Hughes, C.W., Roussenov, V., and Williams R.G.: Meridional coherence of the North Atlantic meridional overturning circulation. *Geophysical Research Letters* 34, 2007.
- Blaauw, M.: Methods and code for 'classical' age-modelling of radiocarbon sequences, *Quaternary Geochronology* 5, 512–518, 2010.
- Bond, G., Kromer, B., Beer, J., Muscheler, R., Evans, M.N., Showers, W., Hoffmann, S., Lotti-Bond, R., Hajdas, I., Bonani, G., 2001. Persistent solar influence on North Atlantic climate during the Holocene. *Science* 294, 2130–2136.
- Brocheray, S., Cremer, M., Zaragosi, S., Schmidt, S., Eynaud, F., Rossignol L., and Gillet, H.: 2000 years of frequent turbidite activity in the Capbreton Canyon (Bay of Biscay), *Marine Geology*, 347, 136–152, doi:10.1016/j.margeo.2013.11.009, 2014.
- Bryden, H. L., Longworth, H. R., and Cunningham, S. A.: Slowing of the Atlantic meridional overturning circulation at 25° N, *Nature* 438, 655–657, 2005.

403 Chabaud, L., Sanchez Goni, M.F., Desprat, S., and Rossignol, L.: Land-sea climatic variability in the
404 eastern North Atlantic subtropical region over the last 14,200 years: Atmospheric and oceanic processes at
405 different timescales, *The Holocene* 24, 787–797, 2014.

406 Charria, G., Lazure, P., Le Cann, B., Serpette, A., Reverdin, G., Louazel, S., Batifoulier, F., Dumas,
407 F., Pichon, A., and Morel Y.: Surface layer circulation derived from Lagrangian drifters in the Bay of
408 Biscay, *Journal of Marine Systems* 109-110, S60–S76. doi:10.1016/j.jmarsys.2011.09.015, 2013.

409 Cisneros, M., Cacho, I., Frigola, J., Canals, M., Masqué, P., Martrat, B., Casado, M., Grimalt, J.O.,
410 Pena, L.D., Margaritelli, G., Lirer, F.: Sea surface temperature variability in the central-western
411 Mediterranean Sea during the last 2700 years: a multi-proxy and multi-record approach. *Climate of the Past*
412 12, 849–869, 2016.

413 Clark, P.U., Pisias, N.G., Stocker, T.F., and Weaver A.J.: The role of the thermohaline circulation in
414 abrupt climate change, *Nature* 415, 863–869, 2002.

415 Copard, K., Colin, C., Henderson, G.M., Scholten, J., Douville, E., Sicre, M.-A., and Frank, N.: Late
416 Holocene intermediate water variability in the northeastern Atlantic as recorded by deep-sea corals, *Earth
417 and Planetary Science Letters*, 313-314, 34–44. doi:10.1016/j.epsl.2011.09.047, 2012.

418 Colin, C., Frank, N., Copard, K., Douville, E.: Neodymium isotopic composition of deep-sea corals
419 from the NE Atlantic: implications for past hydrological changes during the Holocene, *Quaternary Science
420 Reviews*, 29, 2509–2517, doi:10.1016/j.quascirev.2010.05.012, 2010.

421 Dawson, A., Elliott, L., Noone, S., Hickey, K., Holt, T., Wadhams, P., Foster, I.: Historical storminess
422 and climate “see-saws” in the North Atlantic region. *Marine Geology* 210, 247–259, 2004.

423 Debret, M., Bout-Roumazielle, V., Grousset, F., Desmet, M., McManus, J. F., Massei, N., Sebag, D.,
424 Petit, J.-R., Copard, Y., and Trentesaux A.: The origin of the 1500-year climate cycles in Holocene North-
425 Atlantic records. *Climate of the Past* 3, 569–575, 2007.

426 deCastro, M., Gómez-Gesteira, M., Alvarez, I., Gesteira, J.L.G. : Present warming within the context
427 of cooling–warming cycles observed since 1854 in the Bay of Biscay, *Continental Shelf Research*, 29,
428 1053–1059, doi:10.1016/j.csr.2008.11.016, 2009.

429 Desprat, S., Sánchez-Goñi, M.F., Loutre, M.-F.: Revealing climatic variability of the last three
430 millennia in northwestern Iberia using pollen influx data. *Earth and Planetary Science Letters* 213, 63–78,
431 2003.

432 Esnaola, G., Sáenz, J., Zorita, E., Fontán, A., Valencia, V., and Lazare, P.: Daily scale winter-time sea
433 surface temperature variability and the Iberian Poleward Current in the southern Bay of Biscay from 1981 to
434 2010. *Ocean Science Discussions* 9, 3795–3850, 2012.

435 Eynaud, F., Turon, J.L., and Duprat, J.: Comparison of the Holocene and Eemian palaeoenvironments
436 in the South Icelandic Basin: Dinoflagellate cysts as proxies for the North Atlantic surface circulation,
437 *Review of Palaeobotany and Palynology*, 128, 55–79, 2004.

438 Eynaud, F., Rossignol, L., Gasparotto, M.-C.: Planktic foraminifera throughout the Pleistocene: From
439 cell to populations to past marine hydrology. Chapter 8 In "Foraminifera: Classification, Biology, and
440 Evolutionary Significance", edited by: Georgescu, MD, Nova Science Publishers, New York, NY. 2013.

441 Farmer, E.J., Chapman, M.R., and Andrews, J.E.: Holocene temperature evolution of the subpolar
442 North Atlantic recorded in the Mg/Ca ratios of surface and thermocline dwelling planktonic foraminifers,
443 *Global and Planetary Change*, 79, 234–243, 2011.

444 Garcia, J., Mojtahid, M., Howa, H., Michel, E., Schiebel, R., Charbonnier, C., Anschutz, P., and
445 Jorissen F.J.: Benthic and planktic foraminifera as indicators of late glacial to Holocene paleoclimatic
446 changes in a marginal environment: An example from the southeastern Bay of Biscay, *Acta Protozool*, 52,
447 163–182, 2013.

448 Garcia-Soto, C., Pingree, R. D., and Valdés, L.: Navidad development in the southern Bay of Biscay:
449 Climate change and swoddy structure from remote sensing and in situ measurements, *Journal of*
450 *Geophysical Research*, 107, 2002.

451 Garcia-Soto, C. and Pingree, R.D.: Atlantic Multidecadal Oscillation (AMO) and sea surface
452 temperature in the Bay of Biscay and adjacent regions, *Journal of the Marine Biological Association of the*
453 *United Kingdom*, 92, 213–234, 2012.

454 Gaudin, M, Mulder, T., Cirac, P., Berne, S., and Imbert P.: Past and present sedimentation activity in
455 the Capbreton Canyon, southern Bay of Biscay, *Geo-Marine Letters* 26, 331–345, 2006.

456 Giraudeau, J., Jennings, A. E., and Andrews, J.T.: Timing and mechanisms of surface and intermediate
457 water circulation changes in the Nordic Seas over the last 10,000 cal years: a view from the North Iceland
458 shelf, *Quaternary Science Reviews*, 23, 2127–2139, 2004.

459 Giraudeau, J., Grelaud, M., Solignac, S., Andrews, J.T., Moros, M., and Jansen, E.: Millennial-scale
460 variability in Atlantic water advection to the Nordic Seas derived from Holocene coccolith concentration
461 records, *Quaternary Science Reviews*, 29, 1276–1287. doi:10.1016/j.quascirev.2010.02.014, 2010.

462 Guiot, J. and de Vernal, A.: Transfer functions: Methods for quantitative paleoceanography based on
463 microfossils. In: Hillaire-Marcel C. and de Vernal A. (eds), *Proxies in Late Cenozoic Paleoceanography*,
464 Amsterdam: Elsevier, pp. 523–563, 2007.

465 Guiot, J. and de Vernal A.: Is spatial autocorrelation introducing biases in the apparent accuracy of
466 paleoclimatic reconstructions?, *Quaternary Science Reviews*, 30, 1965–1972, 2011.

467 Hatun, H., Britt Sandø, A., Drange, H., Hansen, B. and Valdimarsson, H.: Influence of the Atlantic
468 Subpolar Gyre on the Thermohaline Circulation, *Science*, 309, 1841–1844, 2005.

469 Hayes, A., Kucera, M., Kallel, N., Sbaffi, L. and Rohling, E. J.: Glacial Mediterranean sea surface
470 temperatures based on planktonic foraminiferal assemblages, *Quaternary Science Reviews*, 24, 999–1016,
471 2005.

472 Jackson, L.C., Kahana, R., Graham, T., Ringer, M. A., Woollings, T., Mecking, J. V., and Wood, R.
473 A.: Global and European climate impacts of a slowdown of the AMOC in a high resolution GCM, *Clim
474 Dyn*, 1–18, doi:10.1007/s00382-015-2540-2, 2015.

475 Kennedy, J.J.: A review of uncertainty in in situ measurements and data sets of sea surface
476 temperature, *Reviews of Geophysics*, 52, 1–32, 2014. doi:10.1002/2013RG000434

477 Koutsikopoulos, C., Beillois P., Leroy C., Taillefer F.: Temporal trends and spatial structures of the
478 sea surface temperature in the Bay of Biscay, *Oceanologica Acta*, 21 (2), 335-344, 1998.

479 Kucera, M., Weinelt, M., Kiefer, T., Pflaumann, U., Hayes, A., Weinelt, M., Chen, M.-T., Mix, A.-C.,
480 Barrows, T.T., Cortijo, E., Duprat, J., Juggins, S., and Waelbroeck, C.: Reconstruction of sea-surface
481 temperatures from assemblages of planktonic foraminifera: multi-technique approach based on

482 geographically constrained calibration data sets and its application to glacial Atlantic and Pacific Oceans,
483 Quaternary Science Reviews, 24, 951–998, doi:10.1016/j.quascirev.2004.07.014, 2005.

484 Landsea, C.W., Vecchi, G.A., Bengtsson, L., Knutson, T.R.: Impact of Duration Thresholds on
485 Atlantic Tropical Cyclone Counts*, Journal of Climate, 23, 2508–2519, 2010.

486 Le Cann, B., and Serpette, A.: Intense warm and saline upper ocean inflow in the southern Bay of
487 Biscay in autumn–winter 2006–2007, Continental Shelf Research, 29, 1014–1025,
488 doi:10.1016/j.csr.2008.11.015, 2009.

489 Lherminier, P., and Thierry, V.: The Reykjanes Ridge Experiment, <http://wwz.ifremer.fr>, 2015.

490 Lozier, M.S. and Stewart, N. M., On the Temporally Varying Northward Penetration of Mediterranean
491 Overflow Water and Eastward Penetration of Labrador Sea Water, Journal of Physical Oceanography, 38,
492 2097–2103, 2008.

493 Lozier, M.S., Roussenov, V., Reed, M.S.C. and Williams, R.G.: Opposing decadal changes for the
494 North Atlantic meridional overturning circulation, Nature Geoscience 3, 728–734, 2010.

495 Lozier, M.S.: Overturning in the North Atlantic, Annual Review of Marine Science 4, 291–315, 2012.

496 Magny, M, Bégeot, C, Guiot, J. et al. Contrasting patterns of hydrological changes in Europe in
497 response to Holocene climate cooling phases, Quaternary Science Reviews, 22, 1589-1596, 2003.

498 Mann, M.E., Zhang, Z., Rutherford, S., Bradley, R. S., Hughes, M. K., Shindell, D., Ammann, C.
499 Faluvegi, G. and Ni F.: Global signatures and dynamical origins of the Little Ice Age and Medieval Climate
500 Anomaly, Science, 326: 1256–1260, 2009. *Data available from*
501 http://www.meteo.psu.edu/holocene/public_html/supplements/MultiproxySpatial09/

502 Marchal, O., Cacho, I., Stocker, T.F., Grimalt, J.O., Calvo, E., Martrat, B., Shackleton, N., Vautravers,
503 M., Cortijo, E. and van Kreveld S.: Apparent long-term cooling of the sea surface in the northeast Atlantic
504 and Mediterranean during the Holocene, Quaternary Science Reviews, 21, 455–483, 2002.

505 Martín-Chivelet, J., Muñoz-García, M.B., Edwards, R.L., Turrero, M.J., Ortega, A.I.: Land surface
506 temperature changes in Northern Iberia since 4000yrBP, based on $\delta^{13}\text{C}$ of speleothems. Global and
507 Planetary Change 77, 1–12, 2011.

508 Martrat, B., Grimalt, J.O., Shackleton, N.J., de Abreu, L., Hutterli, M.A. and Stocker, T. F.: Four
509 Climate Cycles of Recurring Deep and Surface Water Destabilizations on the Iberian Margin. *Science* 317,
510 502–507. *Data available from* <http://doi.pangaea.de/10.1594/PANGAEA.771894>, 2007.

511 Mary, Y., Eynaud, F., Zaragosi, S., Malaizé, B., Cremer, M. and Schmidt, S.: High frequency
512 environmental changes and deposition processes in a 2 kyr-long sedimentological record from the Cap-
513 Breton canyon (Bay of Biscay), *The Holocene*, 25, 348–365, doi:10.1177/0959683614558647, 2015.

514 McCartney, M.S., and Mauritzen, C.: On the origin of the warm inflow to the Nordic Seas, *Progress in*
515 *Oceanography*, 51, 125–214, 2001.

516 McGregor, H.V., Evans, M.N., Goosse, H., Leduc, G., Martrat, B., Addison, J.A., Mortyn, P.G., Oppo,
517 D.W., Seidenkrantz, M.-S., Sicre, M.-A., Phipps, S.J., Selvaraj, K., Thirumalai, K., Filipsson, H.L., Ersek,
518 V.: Robust global ocean cooling trend for the pre-industrial Common Era. *Nature Geoscience* 8, 671–677.
519 doi:10.1038/ngeo2510, 2015.

520 Mojtabid, M., Jorissen, F.J., Garcia, J., Schiebel, R., Michel, E., Eynaud, F., Gillet, H., Cremer, M.,
521 Diz Ferreiro, P., Siccha, M., and Howa, H.: High resolution Holocene record in the southeastern Bay of
522 Biscay: Global versus regional climate signals, *Palaeogeography, Palaeoclimatology, Palaeoecology*, 377,
523 28–44. doi:10.1016/j.palaeo.2013.03.004, 2013.

524 Morley, A., Rosenthal, Y., deMenocal, P.: Ocean-atmosphere climate shift during the mid-to-late
525 Holocene transition, *Earth and Planetary Science Letters* 388, 18–26, doi:10.1016/j.epsl.2013.11.039, 2014.

526 Moros, M., Jansen, E., Oppo, D.W., Giraudeau, J., and Kuijpers, A.: Reconstruction of the late-
527 Holocene changes in the Sub-Arctic Front position at the Reykjanes Ridge, north Atlantic, *The Holocene*,
528 22, 877-868, 2012.

529 Naughton, F., Bourillet, J.F., Sanchez Goni, M.-F., Turon J.-L., and Jouanneau J.-M.: Long-term and
530 millennial-scale climate variability in northwestern France during the last 8850 years, *The Holocene*, 17,
531 939–953, 2007a.

532 Naughton, F., Sanchez Goñi, M.F., Desprat, S., Turon, J.-L., Duprat, J., Malaizé, B., Joli, C., Cortijo,
533 E., Drago T. and Freitas, M.C.: Present-day and past (last 25000 years) marine pollen signal off western
534 Iberia, *Marine Micropaleontology*, 62, 91–114, doi:10.1016/j.marmicro.2006.07.006, 2007b.

535 Ollitrault, M. and Colin de Verdière A.: The ocean general circulation near 1000 m depth, *J. Phys.*
536 *Oceanogr.* 44, 384–409, 2014.

537 Oppo, D.W., McManus, J.F., Cullen, J.L.: Deepwater variability in the Holocene epoch. *Nature* 422,
538 277–278, 2003.

539 Peliz, Á., Dubert, J., Santos, A.M.P., Oliveira, P.B., Le Cann, B.: Winter upper ocean circulation in the
540 Western Iberian Basin—Fronts, Eddies and Poleward Flows: an overview, *Deep Sea Research Part I:*
541 *Oceanographic Research Papers*, 52, 621–646, doi:10.1016/j.dsr.2004.11.005, 2005.

542 Pena, L.D., Francés, G., Diz, P., Esparza, M., Grimalt, J.O., Nombela, M.A. and Alejo, I.: Climate
543 fluctuations during the Holocene in NW Iberia: High and low latitude linkages, *Continental Shelf Research*,
544 30, 1487–1496, doi:10.1016/j.csr.2010.05, 2010.

545 Penaud, A., Eynaud, F., Sánchez-Goñi, M.F., Malaizé, B., Turon, J.L., and Rossignol L.: Contrasting
546 sea-surface responses between the western Mediterranean Sea and eastern subtropical latitudes of the North
547 Atlantic during abrupt climatic events of MIS 3, *Marine Micropaleontology*, 80, 1-17, 2011.

548 Pérez-Brunius, P., Rossby, T., Watts, D.R.: Absolute transports of mass and temperature for the North
549 Atlantic Current-Subpolar Front system, *Journal of physical oceanography*, 34, 1870–1883, 2004.

550 Pflaumann, U., Duprat, J., Pujol, C., and Labeyrie, L. D.: SIMMAX: A modern analog technique to
551 deduce Atlantic sea surface temperatures from planktonic foraminifera in deep-sea sediments,
552 *Paleoceanography*, 11, 15–35, 1996.

553 Pingree, R.: North Atlantic and North Sea climate change: curl up, shut down, NAO and ocean colour,
554 *Journal of the Marine Biological Association of the United Kingdom*, 85, 1301–1315, 2005.

555 Pingree, R. D. and Garcia-Soto, C.: Plankton blooms, ocean circulation and the European slope
556 current: Response to weather and climate in the Bay of Biscay and W English Channel (NE Atlantic), *Deep*
557 *Sea Research Part II: Topical Studies in Oceanography*, 106, 5–22, 2014

558 Pingree, R.D. and Le Cann B.: Structure, strength and seasonality of the slope currents in the Bay of
559 Biscay region, *Journal of the Marine Biological Association of the United Kingdom*, 70, 857–885, 1990.

560 Planque, B., Beillois, P., Jégou, A.-M., Lazure, P., Petitgas, P., Puillat, I.: Large-scale hydroclimatic
561 variability in the Bay of Biscay: the 1990s in the context of interdecadal changes, in: ICES Marine Science
562 Symposia, 61–70. 2003.

563 Reimer, P.J., Bard, E., Bayliss, A., Beck, J. W., Blackwell, P. G., Ramsey, C. B., Buck, C. E., Cheng,
564 H., Edwards, R. L., Friedrich, M., Grootes, P. M., Guilderson, T. P., Haflidason, H., Hajdas, I., Hatté, C.,
565 Heaton, T. J., Hoffmann, D. L., Hogg, A. G., Hughen, K. A., Kaiser, K. F., Kromer, B., Manning, S. W.,
566 Niu, M., Reimer, R. W., Richards, D. A., Scott, E. M., Southon, J. R., Staff, R. A., Turney, C. S. M. and
567 van der Plicht, J.: IntCal13 and Marine13 Radiocarbon Age Calibration Curves 0-50,000 Years cal BP,
568 Radiocarbon, 55(4), 2013.

569 Retailleau S., Howa H., Schiebel R., Lombard F., Eynaud F., Schmidt S., Jorissen F., Labeyrie L.:
570 Planktic foraminiferal production along an offshore-onshore transect in the south-eastern Bay of Biscay,
571 Continental Shelf research, 29 (8), 1123-1135, 2009.

572 Retailleau S., Eynaud F., Mary Y., Schiebel R., Howa H.: An Ocean - Canyon head and river plume:
573 how they may influence neritic planktonic foraminifera communities in the SE Bay of Biscay?, Journal of
574 Foraminifera research, 42(3), 257–269, 2012.

575 Risebrobakken, B., Dokken, T., Smedsrud, L.H., Andersson, C., Jansen, E., Moros, M., Ivanova, E.V.:
576 Early Holocene temperature variability in the Nordic Seas: The role of oceanic heat advection versus
577 changes in orbital forcing, Paleoceanography, 26, 2011. doi:10.1029/2011PA002117

578 Rodrigues, T., Grimalt, J.O., Abrantes, F.G., Flores, J.A. and Lebreiro, S.M.:Holocene
579 interdependences of changes in sea surface temperature, productivity, and fluvial inputs in the Iberian
580 continental shelf (Tagus mud patch), Geochemistry, Geophysics, Geosystems 10, n/a–n/a.
581 doi:10.1029/2008GC002367, 2009. Data available from <http://doi.pangaea.de/10.1594/PANGAEA.761812>

582 Roth, R., Joos, F.: A reconstruction of radiocarbon production and total solar irradiance from the
583 Holocene $\delta^{14}\text{C}$ and CO_2 records: implications of data and
584 model uncertainties. Climate of the Past 9, 1879–1909, 2013.

585 Salgueiro, E., Voelker, A., Abrantes, F., Meggers, H., Pflaumann, U., Loncaric, N., Gonzalez-Álvarez,
586 R., Oliveira, P., Bartels-Jónsdóttir, H.B., Moreno, J. and Wefer, G.: Planktonic foraminifera from modern

587 sediments reflect upwelling patterns off Iberia: Insights from a regional transfer function, *Marine*
588 *Micropaleontology* 66, 135–164, 2008.

589 Salgueiro, E., Voelker, A.H.L., de Abreu, L., Abrantes, F., Meggers, H., Wefer, G.: Temperature and
590 productivity changes off the western Iberian margin during the last 150 k^{yr}, *Quaternary Science Reviews*
591 29, 680–695, 2010.

592 Sánchez Goñi, M.F, Bakker, P., Desprat, S., Carlson, A. E., Van Meerbeeck, C. J., Peyron, O.,
593 Naughton, F., Fletcher, W. J., Eynaud, F., Rossignol, L. and Renssen, H.: European climate optimum and
594 enhanced Greenland melt during the Last Interglacial, *Geology*, 40, 627-630, 2012.

595 Sánchez Goñi, M.F., Bard, E., Landais, A., Rossignol, L., d'Errico, F.: Air–sea temperature
596 decoupling in western Europe during the last interglacial–glacial transition, *Nature Geoscience* 6, 837-841,
597 doi:10.1038/ngeo1924, 2013.

598 Sarnthein M., Van Kreveld, S., Erlenkeuser, H., Grootes, P. M., Kucera, M., Pflaumann, U., Schulz,
599 M.: Centennial-to-millennial-scale periodicities of Holocene climate and sediment injections off the western
600 Barents shelf, 75°N , *Boreas*, 32, 447–461, 2003.

601 Schäfer-Neth, C. and Manschke, A., WOA-Sample tool, [http://www.geo.uni-](http://www.geo.uni-bremen.de/geomod/staff/csn/woasample.html)
602 [bremen.de/geomod/staff/csn/woasample.html](http://www.geo.uni-bremen.de/geomod/staff/csn/woasample.html), 2002. last access: January 2016.

603 Staines-Urías, F., Kuijpers, A., and Korte, C.: Evolution of subpolar North Atlantic surface circulation
604 since the early Holocene inferred from planktic foraminifera faunal and stable isotope records. *Quaternary*
605 *Science Reviews* 76, 66–81, 2013.

606 Solignac, S., Grelaud, M., de Vernal, A., Giraudeau, J., Moros, M., McCave N. and Hoogakker, B.:
607 Reorganization of the upper ocean circulation in the mid-Holocene in the Northeastern Atlantic, *Can. J.*
608 *Earth Sci.* 45, 1417-1433, 2008.

609 Sorrel, P., Tessier, B., Demory, F., Delsinne, N., Mouazé, D.: Evidence for millennial-scale climatic
610 events in the sedimentary infilling of a macrotidal estuarine system. *Quaternary Science Reviews* 28 (5–6),
611 499–516, 2009.

612 Sorrel, P., Debret, M., Billeaud I., Jaccard S.L., McManus J.F., and Tessier B.: Persistent non-solar
613 forcing of Holocene storm dynamics in coastal sedimentary archives, *Nature Geoscience* 12, 892–896.
614 doi:10.1038/ngeo1619, 2012.

615 Tanner, B.R., Lane, C.S., Martin, E.M., Young, R. and Collins, B.: Sedimentary proxy evidence of a
616 mid-Holocene hypsithermal event in the location of a current warming hole, North Carolina, USA.
617 *Quaternary Research* 83, 315–323. doi:10.1016/j.yqres.2014.11.004, 2015.

618 Telford, R.J. and Birks, H.J.B.: Effect of uneven sampling along an environmental gradient on
619 transfer-function performance, *Journal of Paleolimnology* 46, 99–106, 2011.

620 Telford, R. J., Li, C., and Kucera M.: Mismatch between the depth habitat of planktonic foraminifera
621 and the calibration depth of SST transfer functions may bias reconstructions, *Climate of the Past*, 9, 859-
622 870, 2013.

623 Thornalley, D. J. R., Elderfield, H. and McCave, I.N.: Holocene oscillations in temperature and
624 salinity of the surface subpolar North Atlantic, *Nature* 457, 711–714, 2009.

625 Trouet V., Scourse, J.D. and Raible, C.C.: North Atlantic storminess and Atlantic Meridional
626 Overturning Circulation during the last Millennium: Reconciling contradictory proxy records of NAO
627 variability, *Global and Planetary Change*, 84–85, 48-55, 2012.

628 Valencia, V., Borja, A., Fontán, A., Pérez, F. F., and Rios, A. F.: Temperature and salinity fluctuations
629 along the Basque Coast (southeastern Bay of Biscay), from 1986 to 2000, related to climatic factors, *ICES*
630 *Journal of Marine Science*, 219: 340-342. 2003.

631 Van Vliet-Lanoe, B., Goslin, J., Hallegouet, B., Henaff, A., Delacourt, C., Fernane, A., Franzetti, M.,
632 Le Cornec, E., Le Roy, P., Penaud, A.: Middle- to late-Holocene storminess in Brittany (NW France): Part I
633 - morphological impact and stratigraphical record, *The Holocene*, 24, 413–433,
634 doi:10.1177/0959683613519687, 2014a.

635 Van Vliet-Lanoe, B., Penaud, A., Henaff, A., Delacourt, C., Fernane, A., Goslin, J., Hallegouet, B., Le
636 Cornec, E.: Middle- to late-Holocene storminess in Brittany (NW France): Part II - The chronology of
637 events and climate forcing, *The Holocene*, 24, 434–453, doi:10.1177/0959683613519688, 2014b.

638 Voelker, A.H.L., de Abreu, L.: A Review of Abrupt Climate Change Events in the Northeastern
639 Atlantic Ocean (Iberian Margin): Latitudinal, Longitudinal, and Vertical Gradients, in: Rashid, H., Polyak,
640 L., Mosley-Thompson, E. (Eds.), Geophysical Monograph Series. American Geophysical Union,
641 Washington, D. C., pp. 15–37, 2011.

642 Wanner, H., Beer J., Bütikofer J., Crowley T.J., Cubasch U., J. Flückiger, H. Goosse, M. Grosjean, F.
643 Joos, J.O. Kaplan, M. Küttel, S.A. Müller, Prentice I.C., Solomina O., Stocker T.F., Tarasov P., Wagner M.
644 and Widmann M.: Mid- to Late Holocene climate change: an overview, *Quaternary Science Reviews* 27,
645 1791–1828. doi:10.1016/j.quascirev.2008.06.013, 2008.

646 Walker, M. J. C., Berkelhammer, M., Björck, S., Cwynar, L. C., Fisher, D. A., Long, A. J., Lowe, J. J.,
647 Newnham, R. M., Rasmussen S. O., and Weiss, H.: Formal subdivision of the Holocene Series/Epoch: a
648 Discussion Paper by a Working Group of INTIMATE (Integration of ice-core, marine and terrestrial
649 records) and the Subcommittee on Quaternary Stratigraphy (International Commission on Stratigraphy),
650 *Journal of Quaternary Science*, 27, 649–659, 2012.

651 Werner, K., Spielhagen, R.F., Bauch, D., Hass, H.C. and Kandiano, E.S.: Atlantic Water advection
652 versus sea-ice advances in the eastern Fram Strait during the last 9 ka: Multiproxy evidence for a two-phase
653 Holocene, *Paleoceanography*, 28(2), 283-295, Data available from
654 <http://doi.pangaea.de/10.1594/PANGAEA.810415>, 2013.

657 **Table caption**

658

659 **Table 1:** Location and references of the southern Bay of Biscay cores used in this study.

660

661 **Table 2:** Summary of AMS ^{14}C ages of core PP10-07 with calendar correspondences.

662

663

<i>Cruise, Core label</i>	<i>Latitude (°N)</i>	<i>Longitude (°E)</i>	<i>Water depth (m)</i>	<i>Longitudinal distance (km) from the shore</i>	<i>Datasources and references</i>
SARGASS, PP10-07	43.677	-2.228	1472	58	This work , Brocheray et al., 2014
PROSECAN IV, KS10b	43.833	-2.050	550	50	This work , Mojtahid et al., 2013
SEDICAR/PICABIA, MD03-2693	43.654	-1.663	431	15	This work , Gaudin et al., 2006, Mary et al., 2015

664

Table 1: Location and references of the southern Bay of Biscay cores used in this study.

665

666

667

668

Depth in core PP10-07 (cm)	Sample	Material	Ref Number	mg C	d ¹³ C	pMC corrected			RAW 14C Age yr BP			corrected reservoir age / -400 yr BP	Calibrated age (median age) CLAM yr BP	-2σ yr	+2σ yr	Error yr	Confidence %
4,5	PP10-07, 3-6 cm (TR1)	Bulk planktonic foraminifera	SacA39103	0,572	0,12	90,6	±	0,24	790	±	30	390	423	353	493	70	92,6
124,5	PP10-07 124-125 cm (TR2)	Bulk planktonic foraminifera	SacA39104	0,455	-1,1	82,1	±	0,24	1590	±	30	1190	1149,5	1063	1236	86,5	95
219,5	PP10-07 218-221	Bulk planktonic foraminifera	SacA 29590	0,7	0,2	77,5	±	0,19	2050	±	30	1650	1618	1533	1702	85	95
380	PP10-07 / 380	Bulk planktonic foraminifera	SacA 26975	0,78	-4,6	72,2	±	0,24	2615	±	30	2215	2271	2175	2366	96	95
720,5	PP10-07 / 720-721	Bulk planktonic foraminifera	SacA 26976	1	-0,9	58,8	±	0,22	4265	±	30	3865	4380	4272	4487	108	95
1050	PP10-07 / 1050	Bulk planktonic foraminifera	SacA 26977	1,1	-5,2	49,4	±	0,17	5660	±	30	5260	6070	5970	6170	100	95
1180	PP10-07 1180	Bulk planktonic foraminifera	SacA 29591	0,69	-0,3	44,6	±	0,14	6490	±	30	6090	7007	6897	7116	110	95
1540	PP10-07 / 1537-1543	Bulk planktonic foraminifera	SacA 26978	1,17	-1,9	33,8	±	0,17	8705	±	40	8305	9371	9276	9466	95	95
1731,5	PP10-07 1730-1733	Bulk planktonic foraminifera	SacA 29592	0,84	-0,8	33	±	0,12	8900	±	30	8500	9556	9477	9635	79	95
1981,5	PP10-07 1980-1983	Bulk planktonic foraminifera	SacA 29593	1	-1,5	31,6	±	0,12	9270	±	30	8870	10093	9992	10193	101	92

669

670

671

Table 2: Summary of AMS ¹⁴C ages of core PP10-07 with calendar correspondences.

672 **Figure caption**

673 **Figure 1: A:** map showing the regional scheme of the main surface currents in the Bay of
674 Biscay, drawn after the compilation of modern hydrological survey from Pingree and Garcia-
675 Soto (2014). North Atlantic Current (NAC), Iberian poleward Current (IPC), and European
676 Slope Current (ESC) are respectively represented by the red and orange arrows. The studied
677 sedimentary cores PP10-07 and KS10b from the inner Bay of Biscay are shown in red.
678 Additional Holocene records cited in the text are displayed by green squares. **B:** North
679 Atlantic general circulation pattern (SPG: Subpolar Gyre, STG: Subtropical Gyre, EPC:
680 European Poleward Current, after Lherminier and Thierry, 2015) with the location of the
681 northern and southern sedimentary records discussed in the text. Core references: **1**-Brocheray
682 et al., 2014; **2**-Mojtahid et al., 2013; **3**-Gaudin et al., 2006; Mary et al., 2015; **4**-Naughton et
683 al., 2007a; **5**-Pena et al., 2010; **6**-Werner et al., 2013; **7**-Sarnthein et al., 2003; **8**-Giraudeau et
684 al., 2004; **9**-Andrews and Giraudeau, 2003; **10**-Thornalley et al., 2009; **11**- Naughton et al.,
685 2007b; **12**-Abrantes et al., 2011; **13**-Chabaud et al., 2014; **14**- Rodrigues et al., 2009; **15**-
686 Martrat et al., 2007; **16**- Risebrobakken et al., 2011; **17**- Cisneros et al., 2016. **C:** SST
687 evolution over the last centuries in the Bay of Biscay (from the MD03-2693 sedimentological
688 record and from the compilation of Garcia-Soto et al., 2002) and comparison, from the top to
689 the bottom with: the Global SST anomaly (after Kennedy, 2014), the Atlantic Tropical
690 Cyclone Counts (after Landsea et al. 2010) and the NAO index of Hurrell
691 (http://research.jisao.washington.edu/data_sets/nao/).

692

693 **Figure 2:** Revised age models for cores KS10b, MD03-2693, and PP10-07 (left panels)
694 compared to previous published age models (right panels with original references).

695

696 **Figure 3:** Mean Annual sea surface temperature (SST) records from the Western European
697 margin. **A:** Holocene SST signals from cores PP10-07 and KS10b (this study) reconstructed
698 using the Modern Analogue Technique (MAT) based on planktonic foraminifera (see
699 Methods), and compared to SST signal of the adjacent core MD03-2693 (Mary et al., 2015).
700 Black dots identify ^{14}C age control points. **B:** SST signals spanning the last 1500 years in the
701 Bay of Biscay (core MD03-2693) based on MAT and from the Iberian Margin (core PO287-
702 06, Abrantes et al., 2011) using alkenones. Reconstructed signals are compared with the AMO
703 reconstruction of Mann et al., (2009). The dotted curve represents core MD03-2693 signal
704 transposed on top of the two other curves. **C:** Holocene SST signals from the Iberian Margin
705 using MAT based on planktonic foraminifera for cores MD99-2331 (after Naughton et al.,
706 2007b) and MD95-2042 (after Chabaud et al., 2014) and Alkenones for cores D13882 (after
707 Rodrigues et al., 2009) and MD01-2444 (after Martrat et al., 2007).

708
709 **Figure 4:** Comparison of annual SST Holocene signals from the Bay of Biscay (**A** and **B**)
710 with records from the northern North Atlantic highlighting variations of the NAC intensity
711 and SPG dynamics; **C:** SST signal of core MSM5/5-712-2 (Fram strait, Werner et al., 2013)
712 and of **D:** core M23258 (Barents shelf, after Sarnthein et al., 2003), both reconstructed using
713 the Modern Analogue Technique (MAT) based on planktonic foraminifera; **E:** Concentration
714 of NAC indicator coccolith species in core MD99-2269 (North Iceland Shelf, after Giraudeau
715 et al., 2004) and in **F:** core B997-330 (North Iceland Shelf, after Andrews and Giraudeau,
716 2003); The PP10-07 record is here also plotted by a thin dotted red line to underline the
717 comparison; **G:** Holocene Storm Periods (after Sorrel et al., 2012) reconstructed from
718 sedimentological evidence from a compilation of coastal cores in North-western Europe; **H:**
719 core Rapid-12-1K (Thornalley et al., 2009) proxy for upper-water column stratification,
720 calculated using derived Mg/Ca and $\delta^{18}\text{O}$ temperatures and salinities of *G. bulloides* and *G.*

721 *inflata*. Dotted vertical lines point out events of density difference between the near-surface
722 and base of the seasonal thermocline in the southern Iceland basin. The topmost dark blue
723 triangles and light blue vertical bands point to cold anomalies recorded in the southern Bay of
724 Biscay (potentially corresponding to a weak SPG).. Pink bands conversely highlight periods
725 of warmth which also correspond to enhanced NAC activity North of Iceland. Changes in
726 gyre circulation dynamics are compared with the Holocene division of Wanner et al. (2008).

727

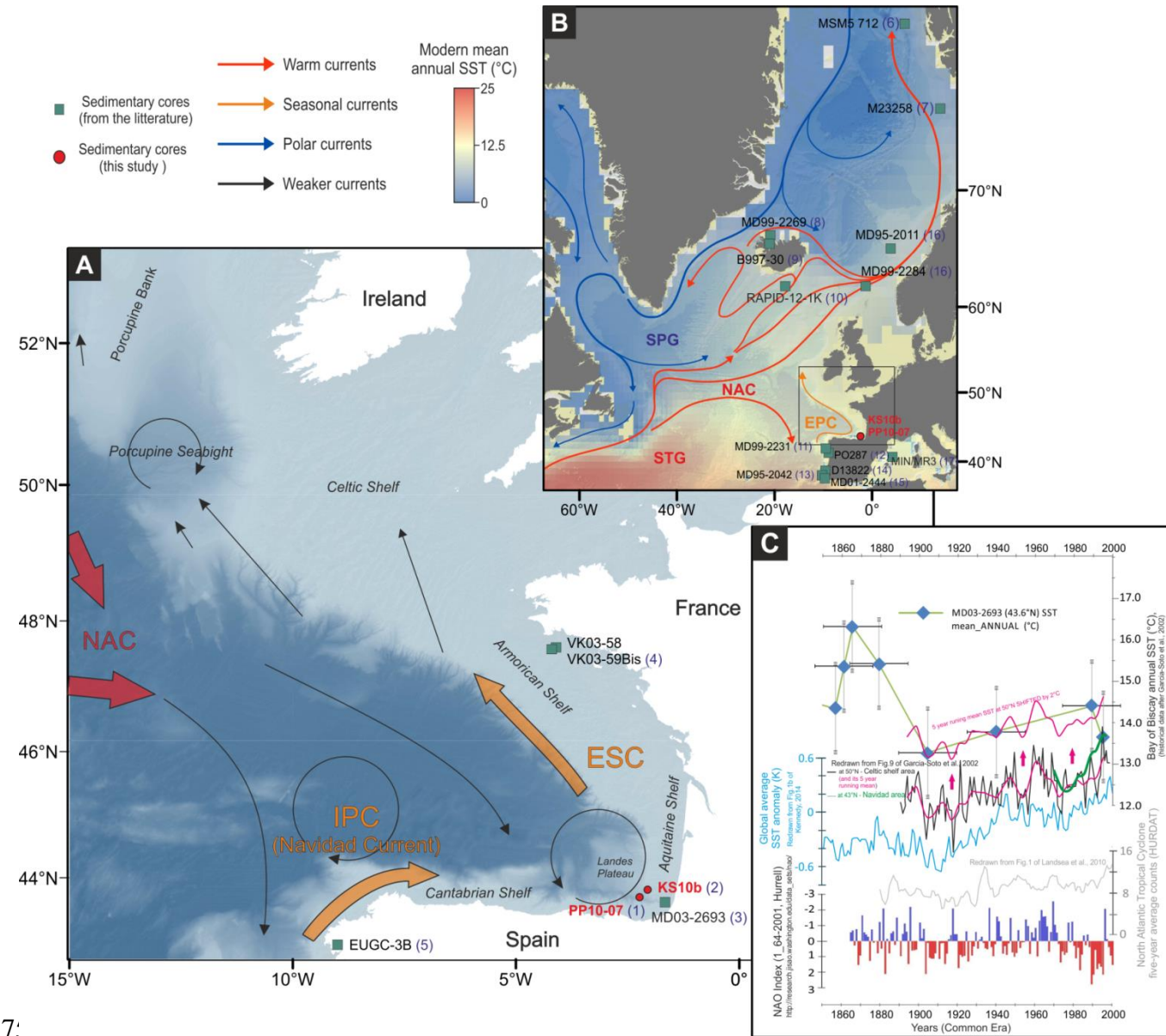
728 **Figure 5:** Gathering data and forcing: comparison of the Bay of Biscay (BB) signals (**A:**
729 annual SST, **B:** XRF ratio in PP10-07, **C:** planktonic foraminifera absolute abundances in
730 PP10-07, **D:** annual SST anomalies vs modern mean in PP10-07), with key Holocene records,
731 i.e.: **E:** Bond et al. 2001 record; **F:** total solar irradiance reconstruction after Roth & Joos,
732 2013; **G:** annual SST anomalies in the Nordic seas (Eastern) digitized from Risebrobakken et
733 al., 2011-Fig3. The dark blue triangles and light blue vertical bands point to cold anomalies
734 recorded in the BB (potentially corresponding to a weak SPG).

735 On the left side are compiled data zooming over the last 4 ka with **A':** BB annual SST; **B':**
736 reconstruction of the European temperature anomalies (from 30-year averages) of the PAGES
737 2k Network (2013); **C':** Cantabrian speleothem $\delta^{13}\text{C}$ stack reflecting 4ka land surface
738 temperature changes, digitized after Martín-Chivelet et al. 2011; **D':** temperate pollen tree
739 influx from the proximal Ria de Vigo, redrawn after Desprat et al., 2003, **E':** Mg/Ca SST
740 anomaly in Minorca and related historical events after Cisneros et al. 2016 (Talaiotic Period -
741 TP, Roman Period -RP, Dark Middle Ages -DMA, Medieval Climate Anomaly -MCA, Little
742 Ice Age -LIA).

743

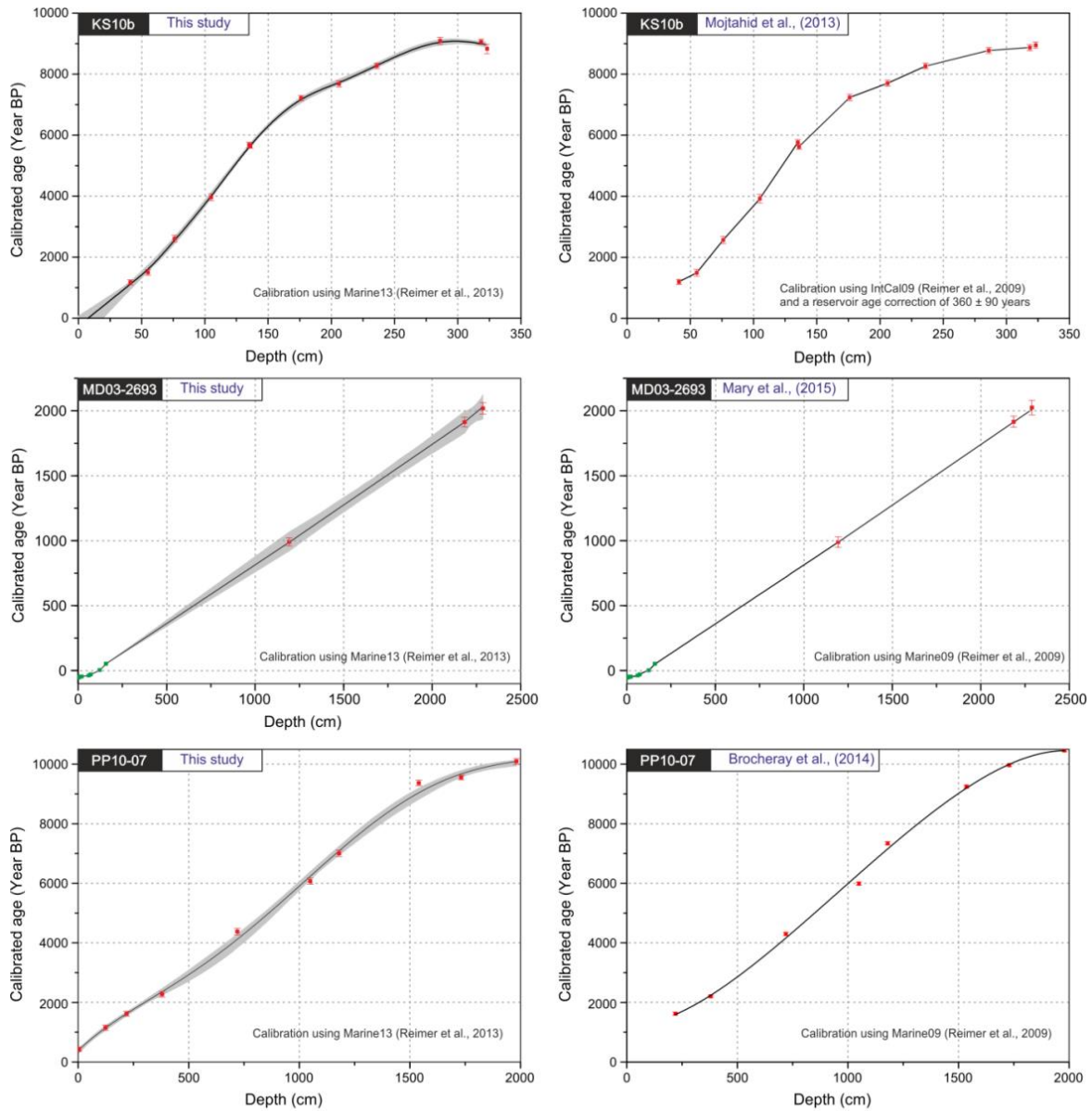
744 **Figure 6:** tentative scheme of North Atlantic oceanic circulation changes associated to
745 contrasted BB SST scenarios (**A:** BB warm anomalies, **B:** BB cool events). This Figure,

746 primarily based on the Figure 1B, was constructed compiling previous works of Staine-Urias
747 et al., 2013 and of Morley et al., 2014 (see also table E2). Squares identify the key records
748 used in Figure 4 and 5 with colors pointed to warm/cool situation or empty when no clear
749 trend is detectable.



7:

Figure 1 (revised)



751

■ ¹⁴C Datings ($\pm 1\sigma$) ■ ²¹⁰Pb Datings ■ Confidence interval

752

753

Figure 2

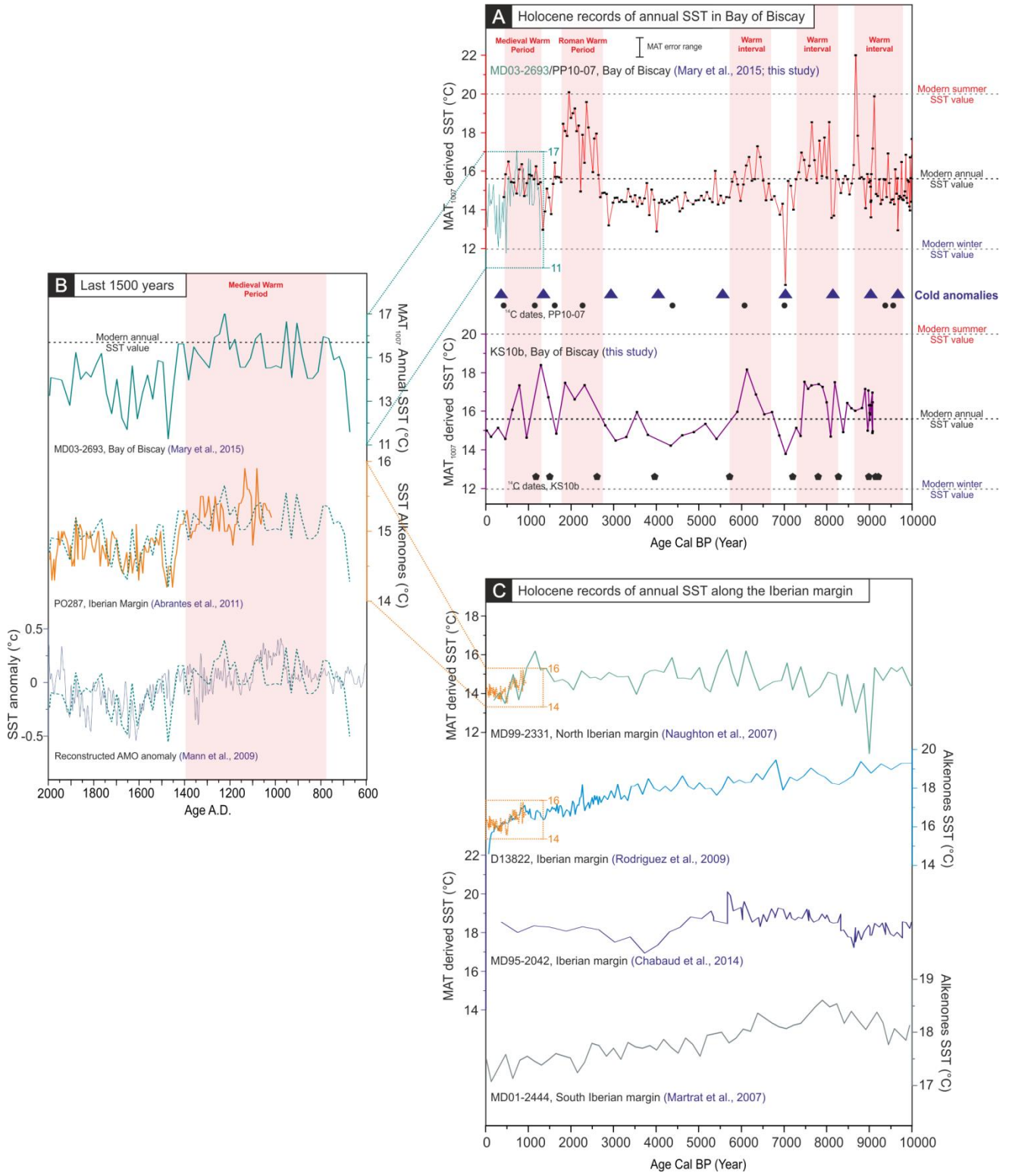


Figure 3

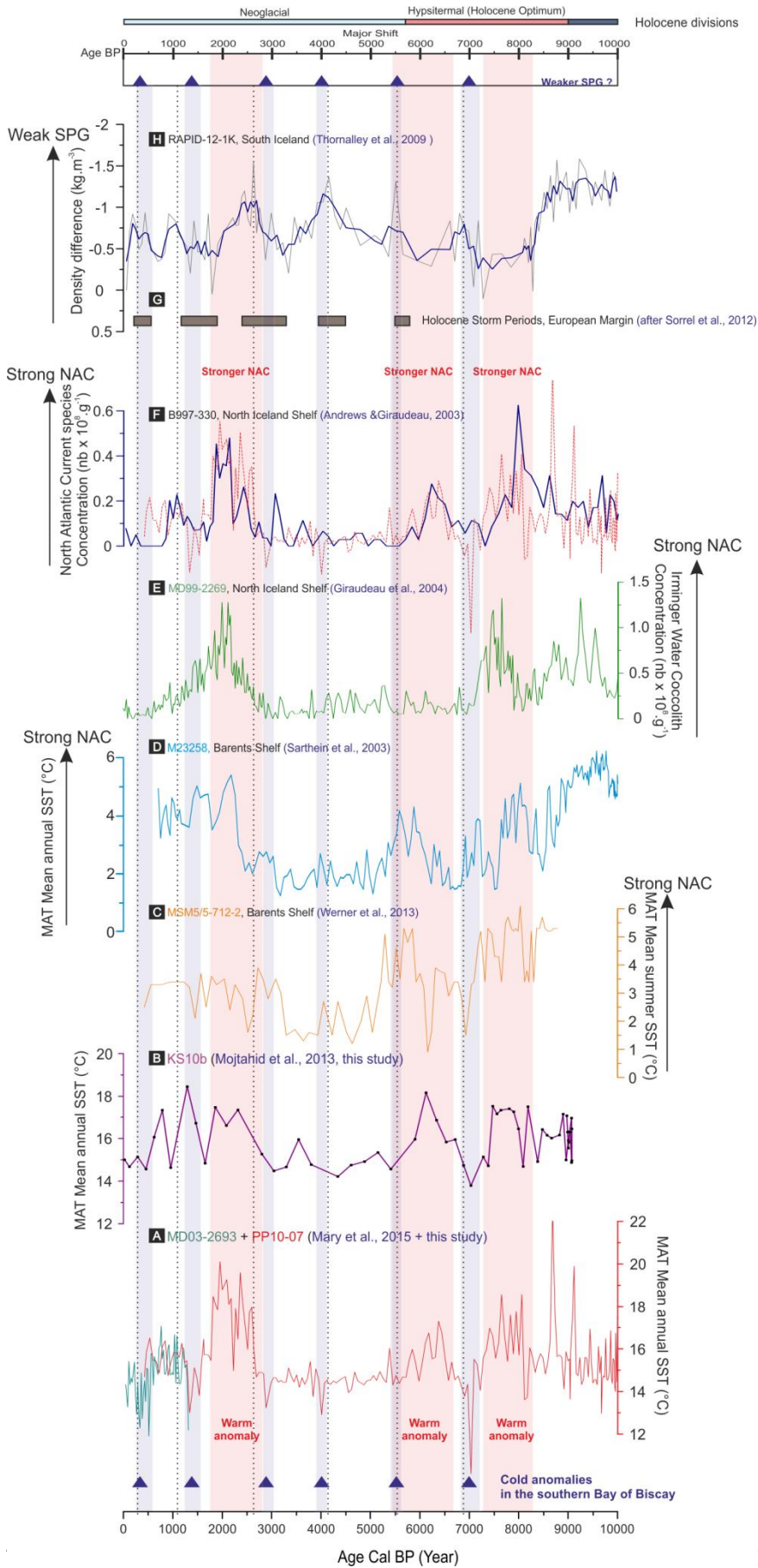
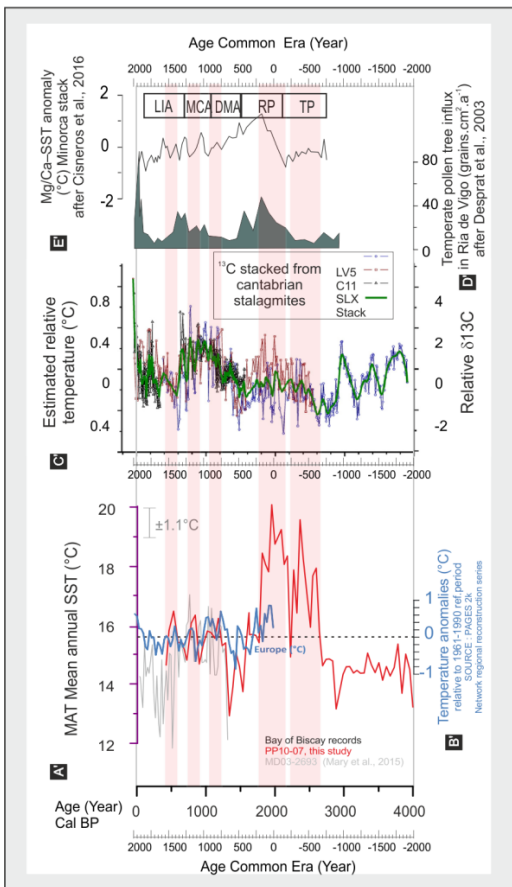
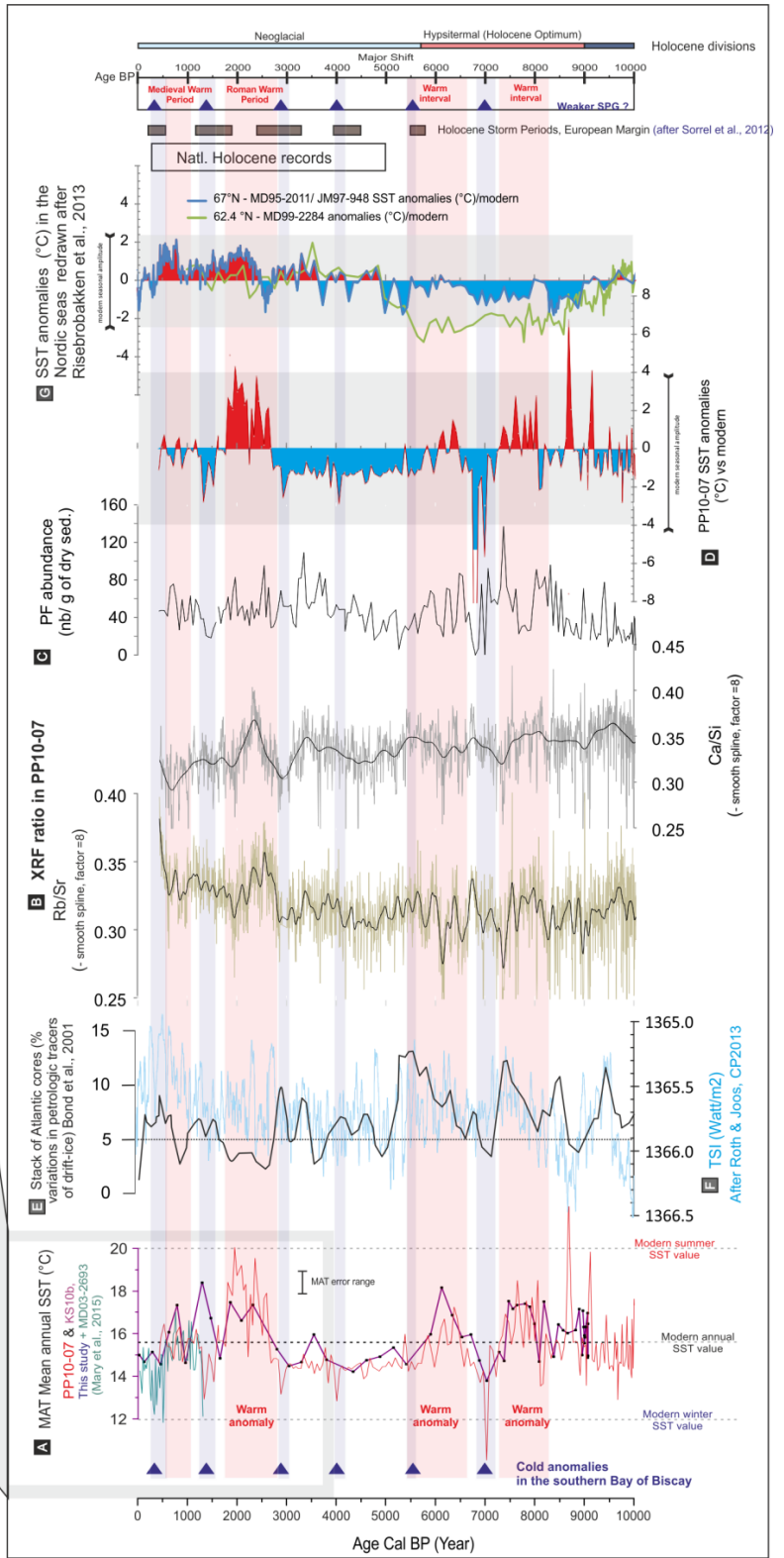


Figure 4



A zoom on the last 4 ka

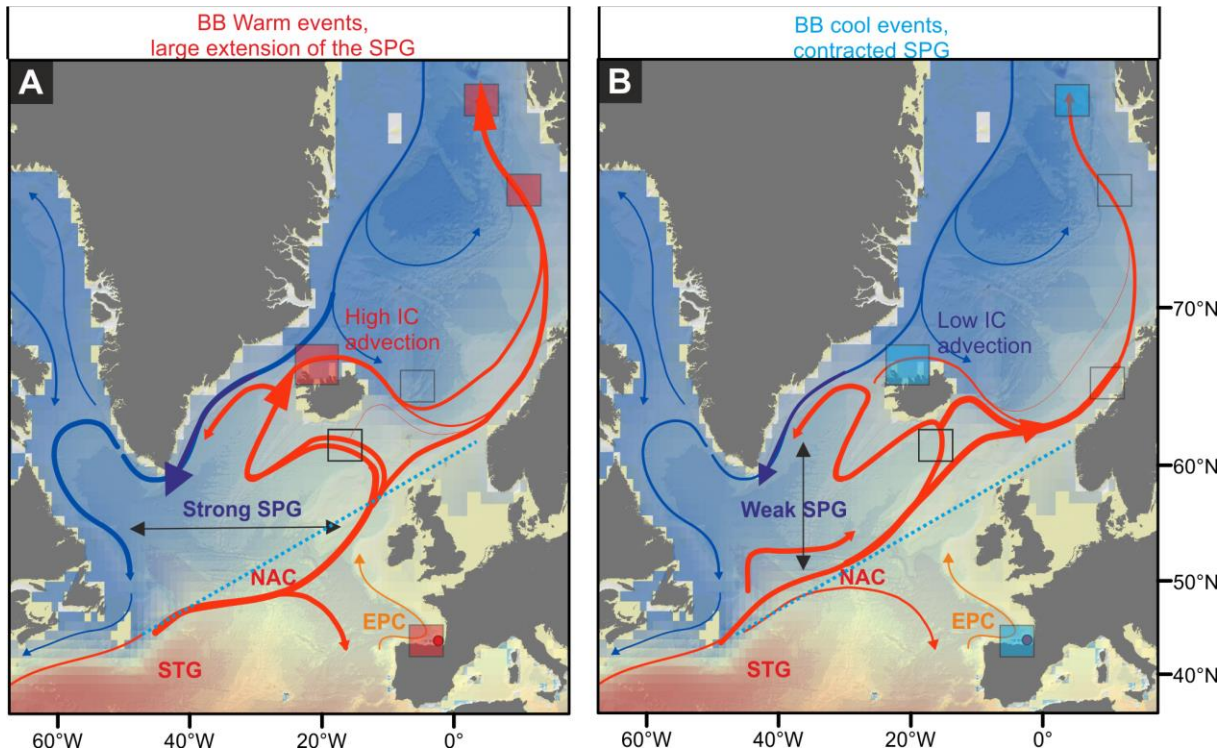


759

760

761

Figure 5



762

763 **Figure 6**